STARS

(**S**patial **T**imeseries for **A**utomated high-**R**esolution multi-**S**ensor data fusion)

Maggie Johnson[1]

Joint work with:

Gregory Halverson[1], Jouni Susiluoto[1], Kerry Cawse-Nicholson[1], Glynn Hulley[1], Joshua Fisher[2]

[1]Jet Propulsion Laboratory, California Institute of Technology

[2]Chapman University

Jet Propulsion Laboratory
California Institute of Technology

STARS

Spatial Timeseries for Automated high-Resolution multi-Sensor data fusion

A new multivariate timeseries-based data fusion method to provide high spatial and temporal resolution products using timeseries of satellite imagery from multiple sensors.

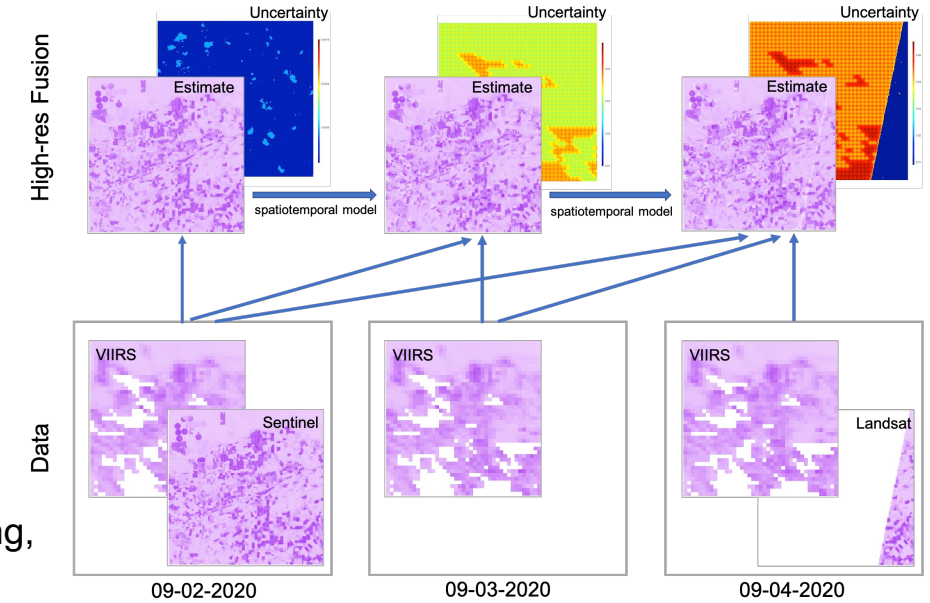

Key features:

- Automated downscaling and spatiotemporal gapfilling
- Uncertainty propagation and quantification
- Computational scalability -- suitable for streaming, post-processing, and offline applications

Major challenge is lack of coincident VSWIR and TIR measurements

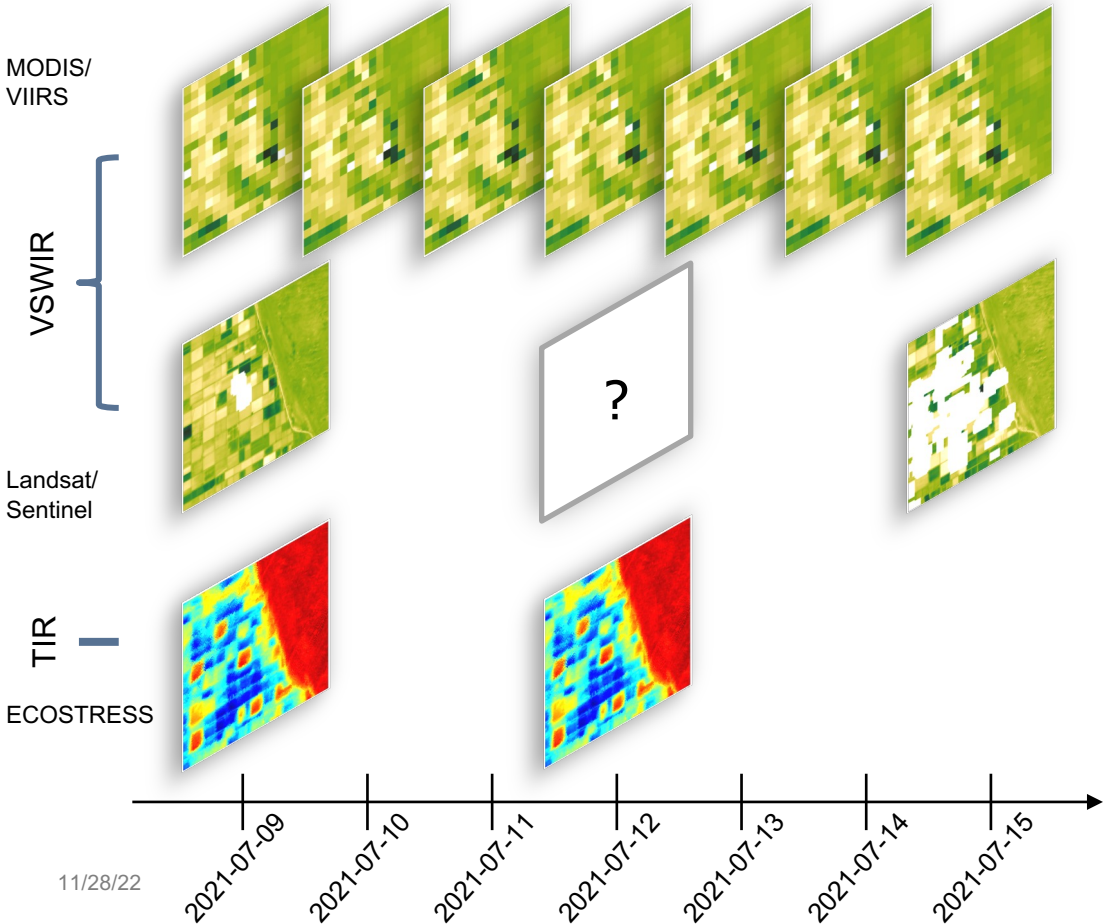

The PT-JPL (Fisher et al., 2009) evapotranspiration (ET) algorithm requires inputs from the visible to shortwave infrared (VSWIR), but VSWIR imagery is rarely coincidently available with ECOSTRESS overpasses at high spatial resolution.

- ≤ 30m resolution weekly+ Sentinel/Landsat is rarely acquired on same day as ECOSTRESS.
- Co-incident daily VIIRS/MODIS (500m - 1km) too coarse to monitor highly heterogenous terrain.

Major challenge is lack of coincident VSWIR and TIR measurements

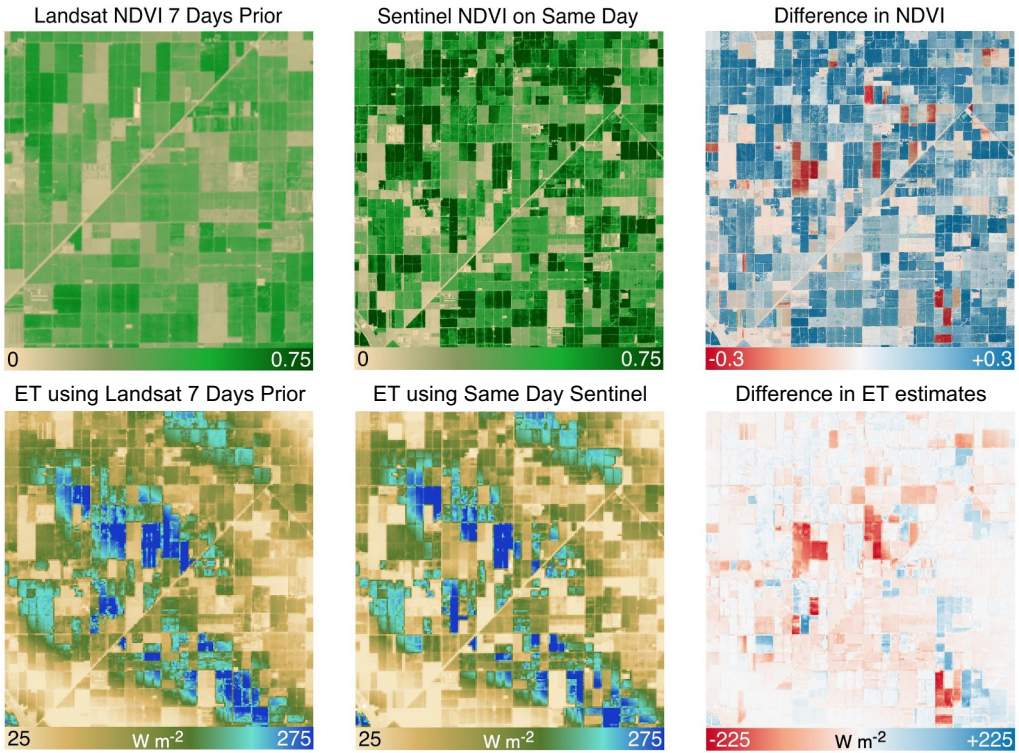

Figure courtesy of G. Halverson.

If substantial phenological change has occurred since last-available high-resolution VSWIR imagery, significant error and uncertainty in ET can result (Cawse-Nicholson, et al. 2020, Halverson et al., in prep).

***STARS** provides the capability to estimate (with uncertainty) coincident NDVI and albedo for any ECOSTRESS overpass.*

Multi-sensor data fusion

Existing Methods (non-exhaustive, see e.g. Zhu et al. 2018 for a review):

- STARFM and subsequent variants (e.g., Gao et al. 2006, Zhu et al. 2010), Unmixing-based methods (e.g., Gevaert, et al. 2011)
- Machine learning, random forests/neural networks (e.g., Yu et al. 2018, Zhang et al. 2018)
- Spatial/spatiotemporal statistical models (e.g., Nguyen, et al. 2012,2014,2017; Ma and Kang, 2020; Johnson, et al., 2021)

Challenges for data fusion

Massive data, mission processing requirements and computational constraints

70m resolution imagery is already ~2million pixels per 100km tile, retrieval algorithms needs to process hundreds of tiles per day (hundreds of tiles per day for ECOSTRESS)!

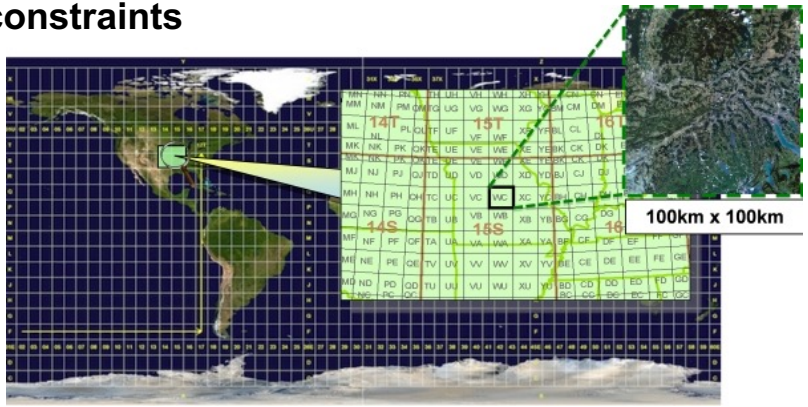

Sentinel 2 100x100km tiling scheme.

Missing data

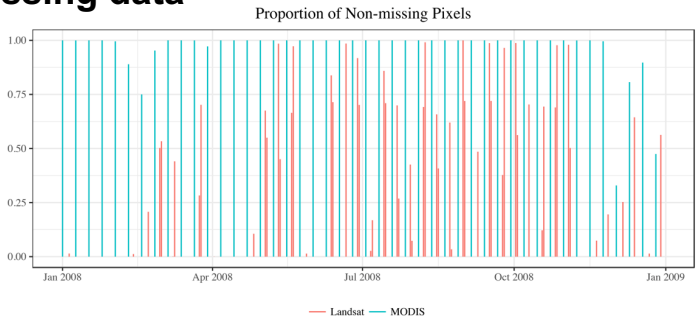

Temporal revisit and cloud contamination can result in no fine spatial imagery over pixels for several days.

Spatial heterogeneity

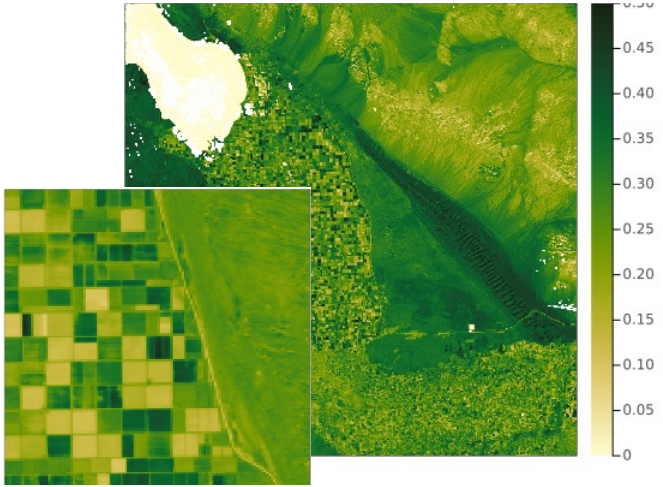

Land surface properties (e.g. fields) exhibit sharp structural change not easily modeled by smooth spatial processes.

Uncertainty Quantification!

Multi-sensor data fusion

Existing Methods (non-exhaustive, see e.g. Zhu et al. 2018 for a review):

- STARFM and subsequent variants (e.g., Gao et al. 2006, Zhu et al. 2010), Unmixing-based methods (e.g., Gevaert, et al. 2011)
- Machine learning, random forests/neural networks (e.g., Yu et al. 2018, Zhang et al. 2018)
- Spatial/spatiotemporal statistical models (e.g., Nguyen, et al. 2012,2014,2017; Ma and Kang, 2020; Johnson, et al., 2021)

Our Approach:

Leverage probabilistic time series models, learn how high resolution imagery evolves through time using coarse resolution imagery

- Model with spatially local, space-time dynamic linear models (e.g. Cressie and Wikle, 2011)
  - Provides means for uncertainty propagation and quantification
- Computational scalability and spatial nonstationarity through approximate, moving window Kalman filtering/smoothing

Dynamic linear models

General model formulation

$$\boldsymbol{Y}_t = \boldsymbol{F}_t \boldsymbol{x}_t + \boldsymbol{v}_t, \qquad \boldsymbol{v}_t \sim N(\boldsymbol{0}, \boldsymbol{V}_t)$$
$$\boldsymbol{x}_t = \boldsymbol{G}_t \boldsymbol{x}_{t-1} + \boldsymbol{\omega}_t, \qquad \boldsymbol{\omega}_t \sim N(\boldsymbol{0}, \boldsymbol{W}_t)$$

- $\boldsymbol{Y}_t$ -- n_t dim vector of observations at time $t = 1, \ldots, T$
- $\boldsymbol{x}_t$ -- p dim vector of latent states (e.g. high resolution imagery) at time *t*
- $\boldsymbol{F}_t$ -- observation matrix defines how observations relate to state process
- $\boldsymbol{G}_t$ -- transition matrix defines how states evolve in time
- $\{\boldsymbol{v}_t\}$ and $\{\boldsymbol{\omega}_t\}$ are Gaussian white noise processes

State estimation

- Filtering: $p(x_t|y_{1:s}),\ \ s = t$
- Smoothing: $p(x_t|y_{1:s}),\ s > t$

Efficient evaluation via Kalman filtering/smoothing recursions (Kalman, 1960) – only requires propagation of mean and covariance matrices.

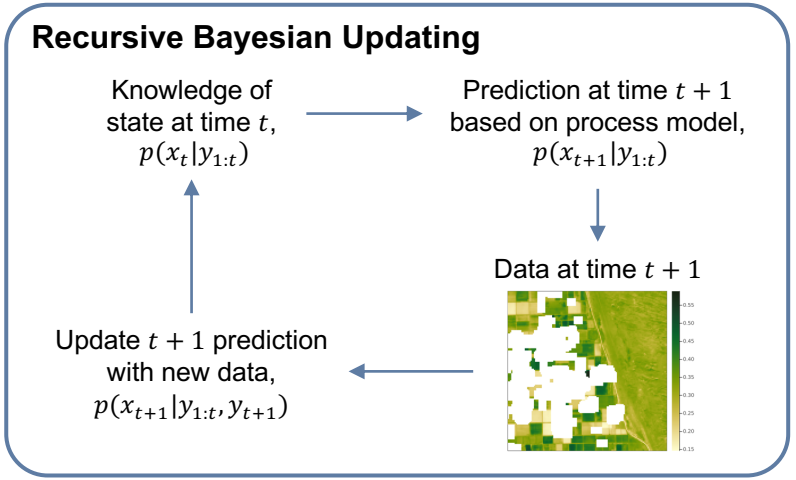

Measurement model

Target Process

$\{x_t(s_i): i = 1, \dots, n\}$ -- latent true process defined on a target, high resolution grid made up of n non-overlapping pixels with centroid locations s_i

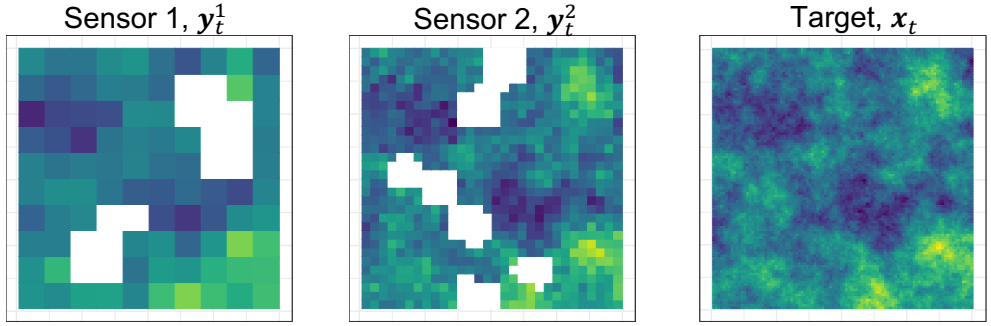

Spatial change of support

Assume the measurement in the k-th instrument grid, at pixel G^k is a noisy, potentially biased, aggregate of the true process (spatial change of support)

$$y_t^k(G^k) = \alpha_t^k(G^k) + \sum_{i=1}^{n} w_i^k \, x_t(s_i) + v_t^k(G^k), \qquad v_t^k(G^k) \sim N(0, V_t^k(G^k))$$

where

- $y_t^k(G^k)$ -- measurement from instrument k in grid cell G^k on day t
- $\alpha_t^k(G^k)$ -- additive dynamic bias for instrument k
- w_i^k -- aggregate weights, typically assumed uniform (simple average)

For a collection of pixels:

$\boldsymbol{F_t}$ -- aggregation matrix

$\boldsymbol{V_t}$ -- diagonal measurement error for each instrument

Process model

Assume states $\boldsymbol{x}_t$ for a collection of high-resolution pixels $i = 1, \dots, n_f$, are spatially-correlated timeseries

$$\boldsymbol{x}_t = \boldsymbol{x}_{t-1} + \boldsymbol{\omega}_t, \qquad \boldsymbol{\omega}_t \sim N(0, \boldsymbol{\Omega}_t)$$

where

- $\boldsymbol{x}_t = \left(x_{1t}, \dots, x_{n_f t}\right)'$ for $t = 1, \dots, T$ and $\boldsymbol{\Omega}_t$ is $n_f \, x \, n_f$ covariance matrix

Models for $\boldsymbol{\Omega}_t$ (increasing in complexity and performance):

1. Independence between pixels ($\boldsymbol{\Omega}_t = \sigma^2 \boldsymbol{I}$) → *ECOSTRESS Collection 2*
   - Very computationally efficient, can be prone to coarse resolution artifacts for long lags between fine resolution imagery
2. Correlation based on spatial distance
   - Gaussian processes and graphical models, eliminates spatial artifacts with smooth downscaling
3. Correlation based on historically similar timeseries/landcover
   - Captures field level similarity, requires availability of long-run timeseries or landcover information

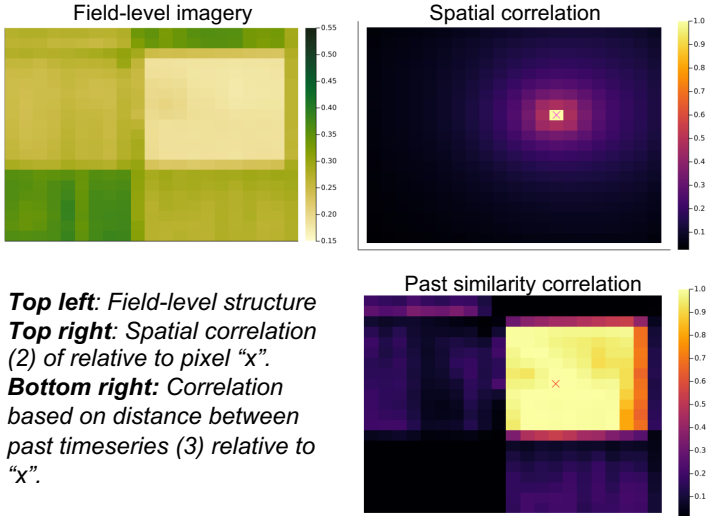

***Top left**: Field-level structure*
***Top right**: Spatial correlation (2) of relative to pixel "x".*
***Bottom right:** Correlation based on distance between past timeseries (3) relative to "x".*

Fusion via Kalman filtering/smoothing

Given the model specification, the fusion targets are the posterior distributions $\boldsymbol{x}_t|\boldsymbol{y}_{1:t} \sim N(\boldsymbol{m}_t, \boldsymbol{C}_t)$ (filtering) or $\boldsymbol{x}_t|\boldsymbol{y}_{1:T} \sim N(\boldsymbol{s}_t, \boldsymbol{S}_t)$ (smoothing) obtained via Kalman recursions

- $\boldsymbol{m}_t/\boldsymbol{s}_t$ and $\boldsymbol{C}_t/\boldsymbol{S}_t$ provide the fused estimate and associated uncertainty

Moving window implementation

Fuse on small overlapping windows defined on a "super-grid", iterate across the target domain.

Given defined moving window super-grid, for each cell:

1. Select all instrument observations within a specified buffer
2. Obtain filtered/smoothed distributions for n_f pixels within window
3. Retain fused estimates only within super-grid cell, discard extra pixels within buffer region

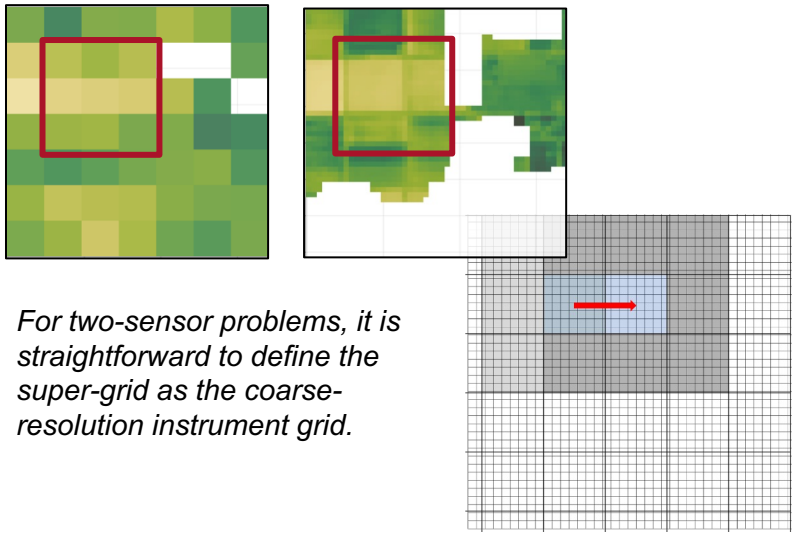

For two-sensor problems, it is straightforward to define the super-grid as the coarse-resolution instrument grid.

Computational cost scales with buffer window size as $\mathcal{O}(n_f^3)$

Near-infrared (NIR) surface reflectance data

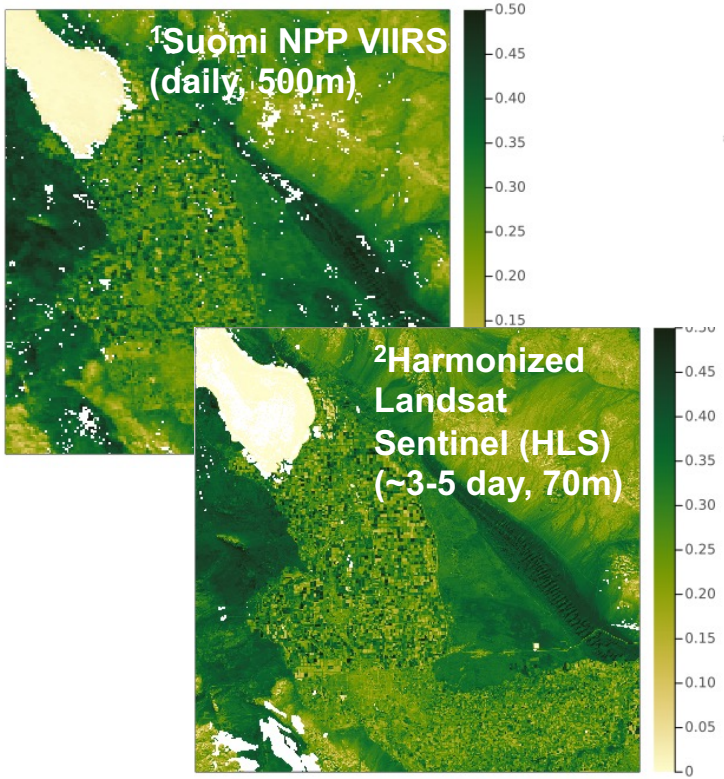

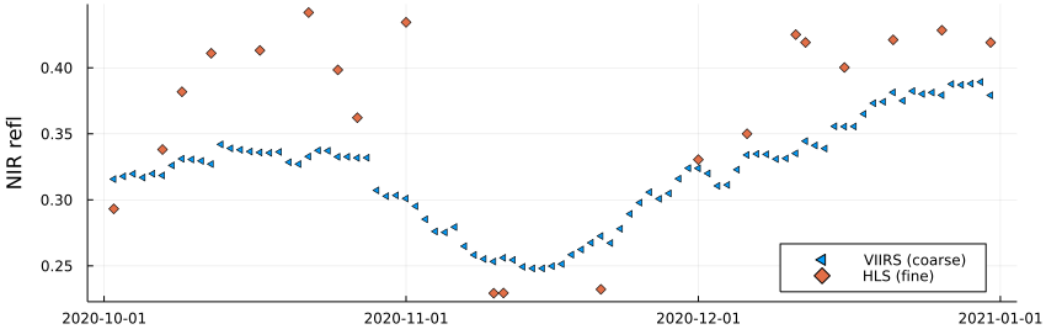

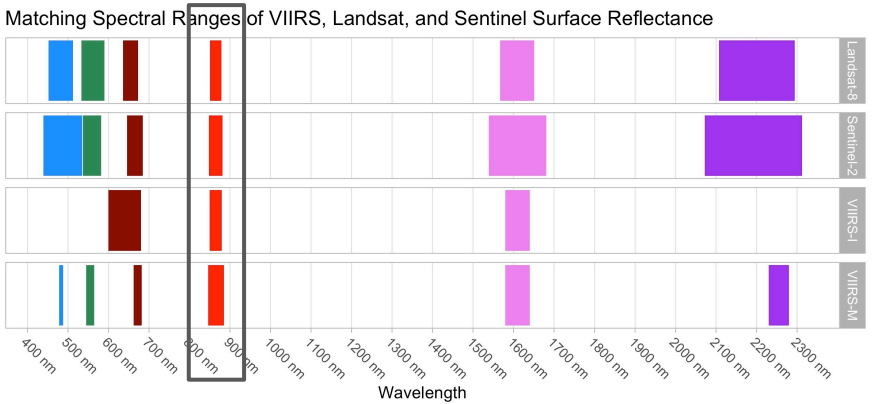

[1]Schaaf et al., 2018, https://lpdaac.usgs.gov/products/vnp43ia3v001/
[2]Claverie, et al, 2018, https://hls.gsfc.nasa.gov/

Example results Salton Sea, CA

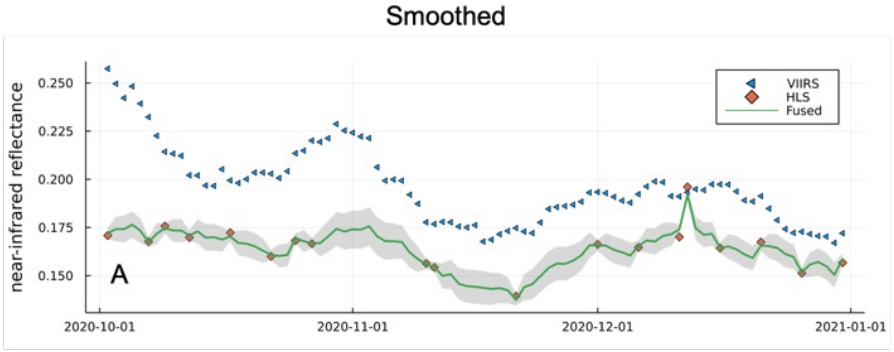

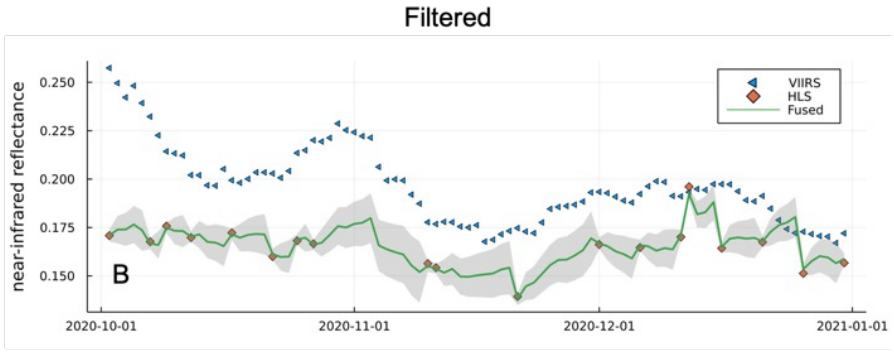

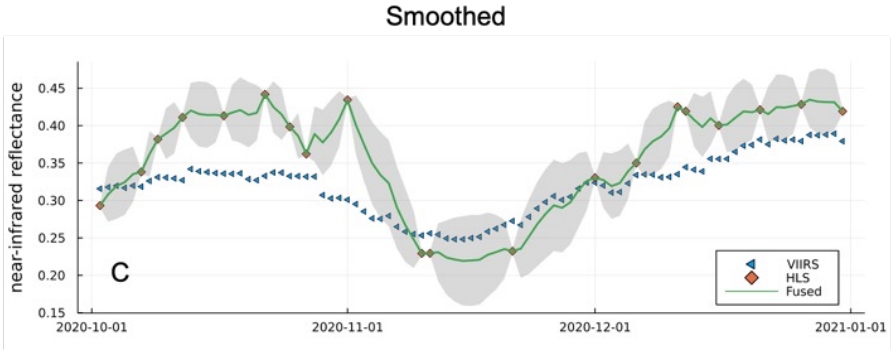

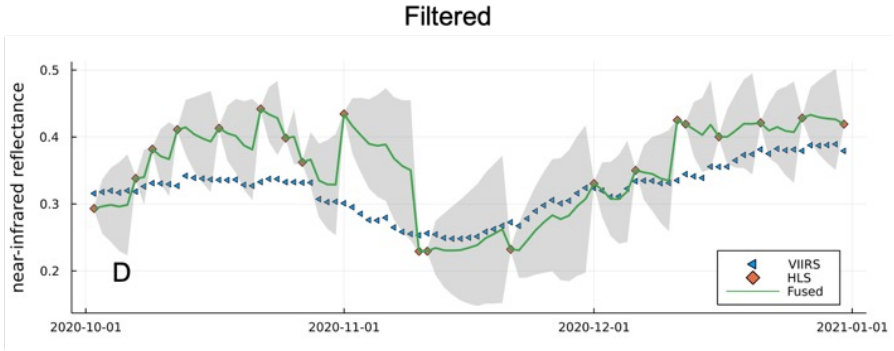

Example results Salton Sea, CA

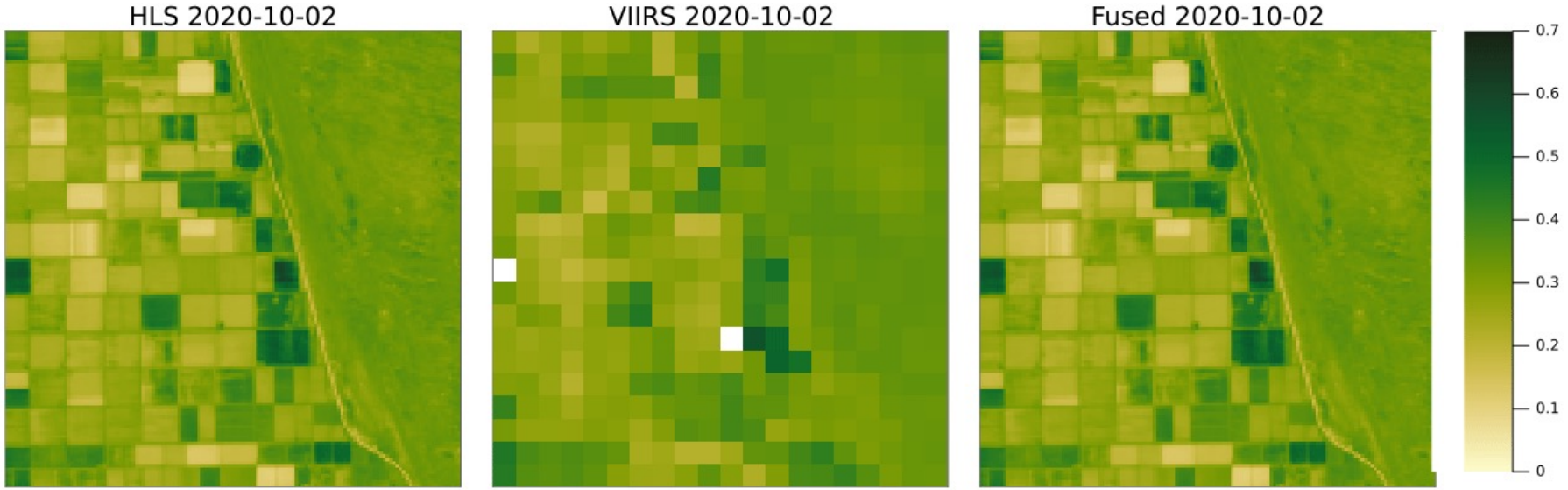

Daily, 70m smoothed fused estimates (using past and future data) from Oct. 01 – Dec 31, 2020.

Example results Salton Sea, CA

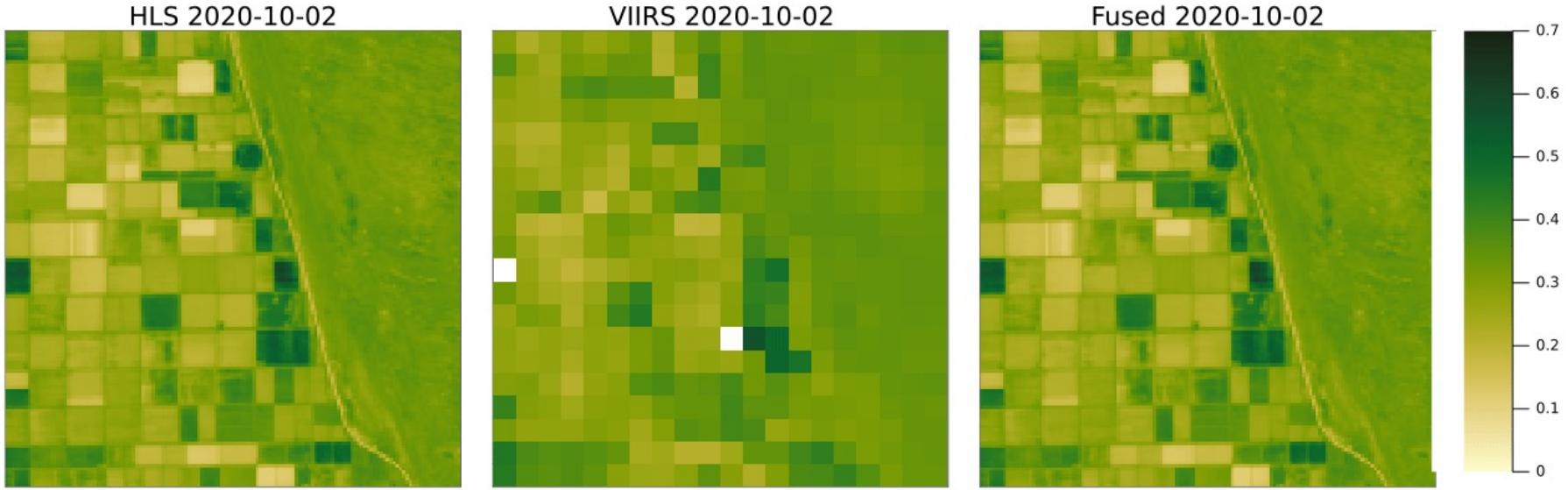

Daily, 70m Filtered fused estimates (using past and future data) from Oct. 01 – Dec 31, 2020.

Performance Assessment

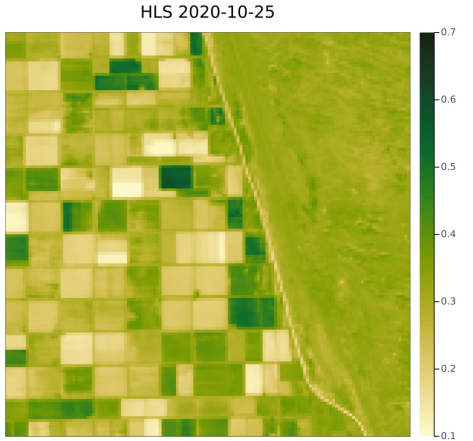

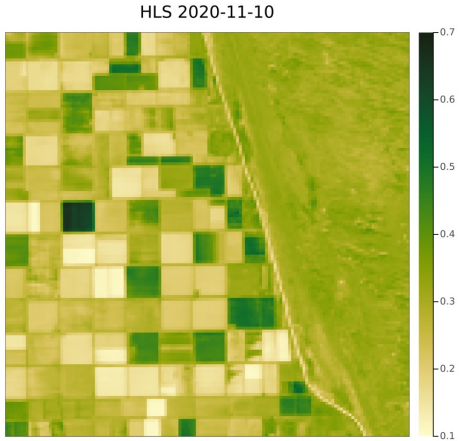

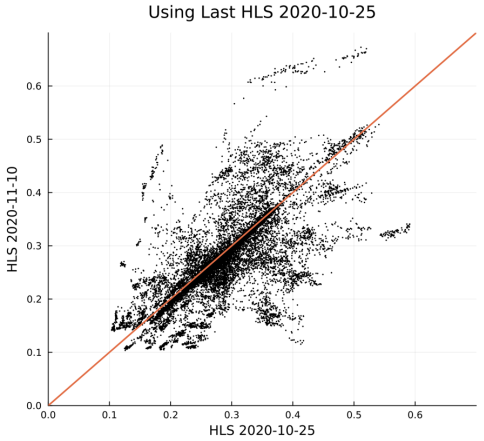

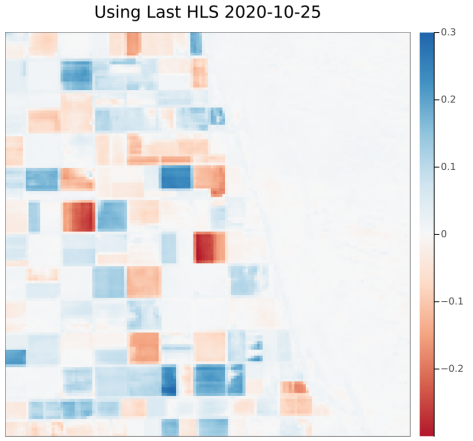

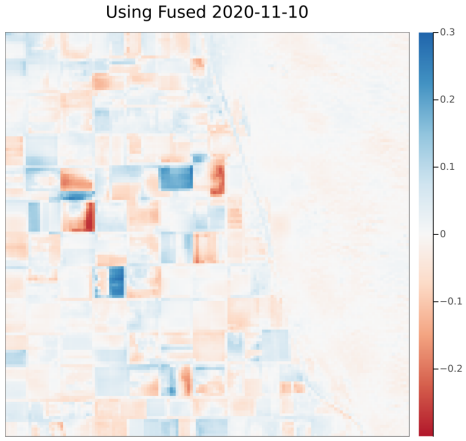

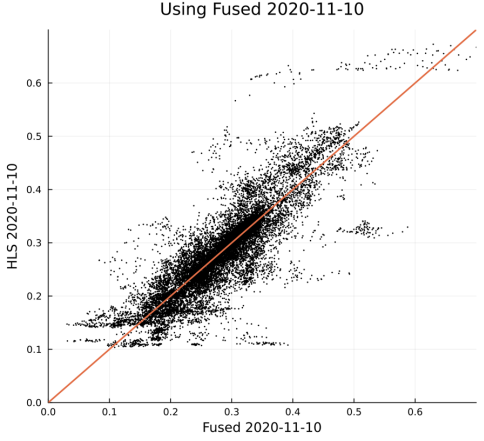

Example fusion HyTES region UK

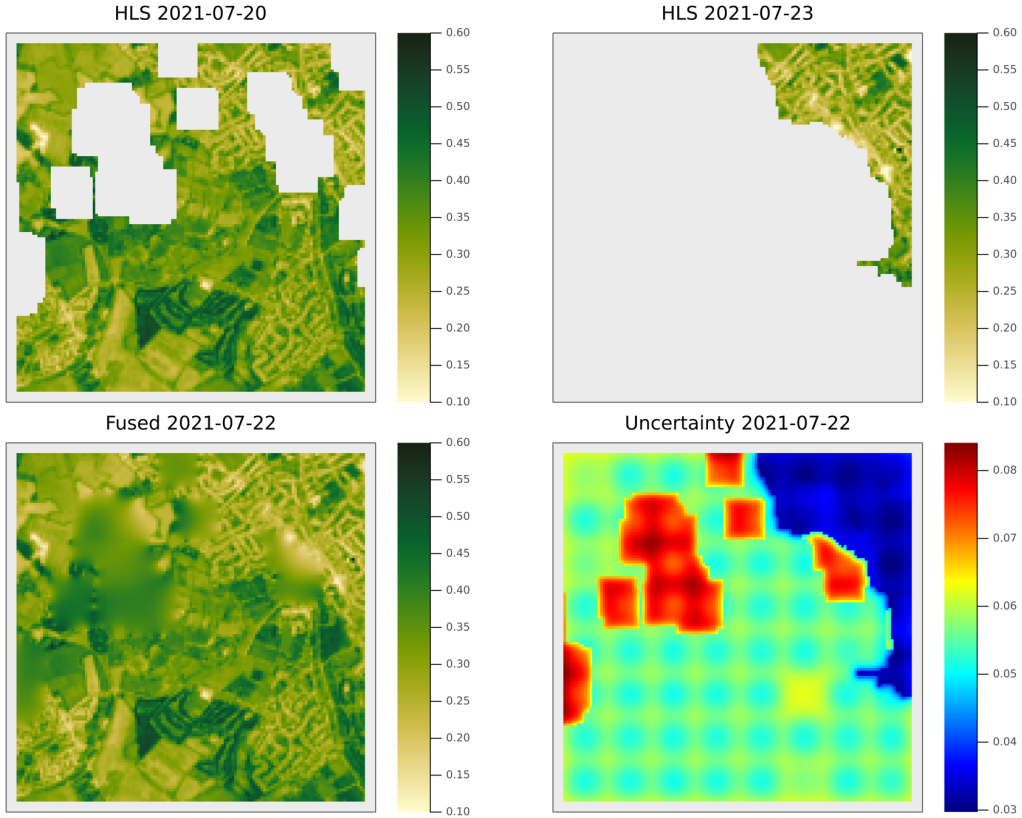

Example fusion results on July 22, 2021 over the HyTES testbed region. (Top) Most recently available 30m HLS imagery to the target date July 20, 2021 and July 23, 2021. (Bottom) 30m resolution fused imagery (left) with estimated pixel-level uncertainties (right) using all available HLS/VIIRS data from July 5 – August 4, 2021.

Summary

The STARS algorithm provides the capability to produce spatiotemporally complete imagery with associated uncertainty estimates at high spatial and temporal resolution.

- An initial version of STARS (independence model) has been integrated into the ECOSTRESS Collection 2 pipeline to produce coincident NDVI and albedo for the PT-JPL ET algorithm.

- STARS development is ongoing, we are currently working on automated approaches to specify/estimate model parameters, additional tricks for computational scalability, etc.

- Our aim is for the improved and generalized STARS methods to be available and suitable for any future ECOSTRESS reprocessing, SBG, and many other applications.

Thank You!

Contact: maggie.johnson@jpl.nasa.gov

Acknowledgements

This work was performed at the Jet Propulsion Laboratory, California Institute of Technology, under contract with the National Aeronautics and Space Administration.

References

- Claverie, M., et al., (2018). The Harmonized Landsat and Sentinel-2 surface reflectance data set. *Remote Sensing of Environment*, 219, 145-161.
- Cressie, N. and Wikle, C. K. (2015) Statistics for spatio-temporal data. John Wiley & Sons.
- Gao, F., et al. (2006). On the blending of the Landsat and MODIS surface reflectance: Predicting daily Landsat surface reflectance. *IEEE Transactions on Geoscience and Remote Sensing*, 44, 2207–2218.
- Johnson, M., et al., (2021). Multisensor fusion of remotely sensed vegetation indices using space-time dynamic linear models. *Journal of the Royal Statistical Society, Series C*, 70, 793-812.
- Ma, P., and Kang, E. L., (2020). Spatiotemporal data fusion for massive sea surface temperature data from MODIS and AMSR-E instruments. *Environmetrics*. 2020; 31, e2594.
- Nguyen, H., et al., (2012). Spatial statistical data fusion for remote sensing applications. *Journal of the American Statistical Association*, 107, 1004–1018.
- Nguyen, H., et al., (2014). Spatiotemporal data fusion for very large remote sensing datasets. *Technometrics*, 56, 174–185.
- Nguyen, H., et al., (2017). Multivariate spatial data fusion for very large remote sensing datasets. *Remote Sensing*, 9, 142.
- Schaaf, C., et al., (2018). *VIIRS/NPP BRDF/Albedo Albedo Daily L3 Global 500m SIN Grid V001* [Data set]. NASA EOSDIS Land Processes DAAC.
- Yu, L., et al., (2019). High-Resolution Global Contiguous SIF of OCO-2. Geophysical Research Letters 46:1449–1458.
- Zhang, Y., Joiner, J., Gentine, P. and Zhou, S. (2018), Reduced solar-induced chlorophyll fluorescence from GOME-2 during Amazon drought caused by dataset artifacts. Glob Change Biol, 24: 2229-2230.
- Zhu, X., et al., (2018). Spatiotemporal fusion of multisource remote sensing data: Literature survey, taxonomy, principles, applications, and future directions. *Remote Sensing*, 10.

Jet Propulsion Laboratory
California Institute of Technology

jpl.nasa.gov